Electronic Supporting Information

Toxic, Radioactive, and Disordered: A Total Scattering Study of $TlTcO_4$

Bryce G. Mullens,[1] Frederick P. Marlton,[2] Matilde Saura-Múzquiz,[3] Michelle Everett,[4] Cheng Li,[4] Alicia M. Manjon-Sanz,[4] Matthew G. Tucker,[4] Frederic Poineau,[5] James Louis-Jean,[5] Supratik Mukherjee,[6] Subrata Mondal,[6] Ganapathy Vaitheeswaran,[7,*] and Brendan J. Kennedy[1,*]

[1] School of Chemistry, The University of Sydney, Sydney, New South Wales 2006, Australia.

[2] Centre for Clean Energy Technology, School of Mathematical and Physical Sciences, Faculty of Science, University of Technology Sydney, Sydney, New South Wales 2007, Australia.

[3] Departamento de Física de Materiales, Facultad de Ciencias Físicas, Universidad Complutense de Madrid, 28040, Madrid, Spain.

[4] Neutron Scattering Division, Oak Ridge National Laboratory, Oak Ridge, Tennessee 37831, USA.

[5] Department of Chemistry, University of Nevada Las Vegas, Las Vegas, Nevada, 89154, USA.

[6] Advanced Centre of Research in High Energy Materials (ACRHEM), University of Hyderabad, Prof. C. R. Rao Road, Gachibowli, 500046 Hyderabad, Telangana, India.

[7] School of Physics, University of Hyderabad, Prof. C. R. Rao Road, Gachibowli, 500046 Hyderabad, Telangana, India.

* Corresponding Authors: Brendan J. Kennedy (brendan.kennedy@sydney.edu.au) and Ganapathy Vaitheeswaran (vaithee@uohyd.ac.in)

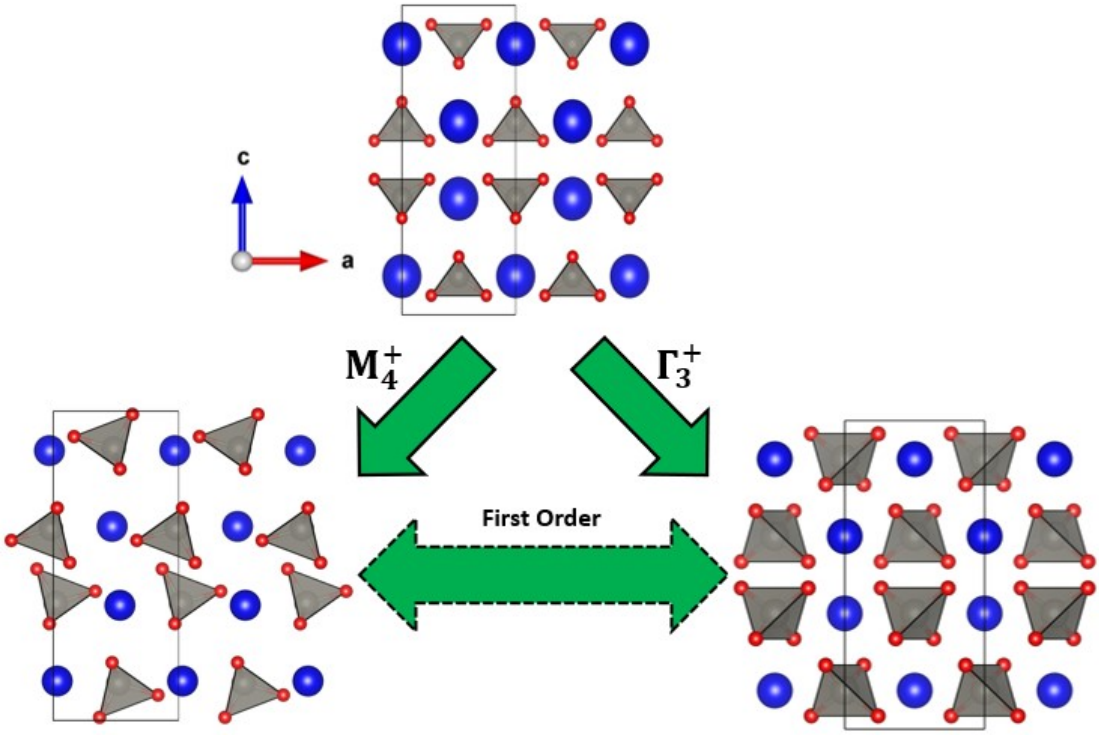

Figure S1: Relationship between the scheelite-type aristotype $I4_1/amd$ and the orthorhombic *Pnma* and tetragonal $I4_1/a$ structures. Each transition is governed by a particular mode, namely the M_4^+ governing rotations of the BO_4 tetrahedra around the *b* axis, and Γ_3^+ governing rotations of the BO_4 tetrahedra around the *c* axis.

Savitzky-Golay Filtering of Neutron Pair Distribution Function Data:

A Savitzky-Golay filter was used on the neutron powder diffraction data of $TlTcO_4$ collected on POWGEN at the Spallation Neutron Source of Oak Ridge National Laboratory. This filter was used to smooth the $S(Q)$ without distorting the signal of the data.

For the 50 K dataset, the Savitzky-Golay filter was applied to $Q \geq 17.0$ Å^{-1}.

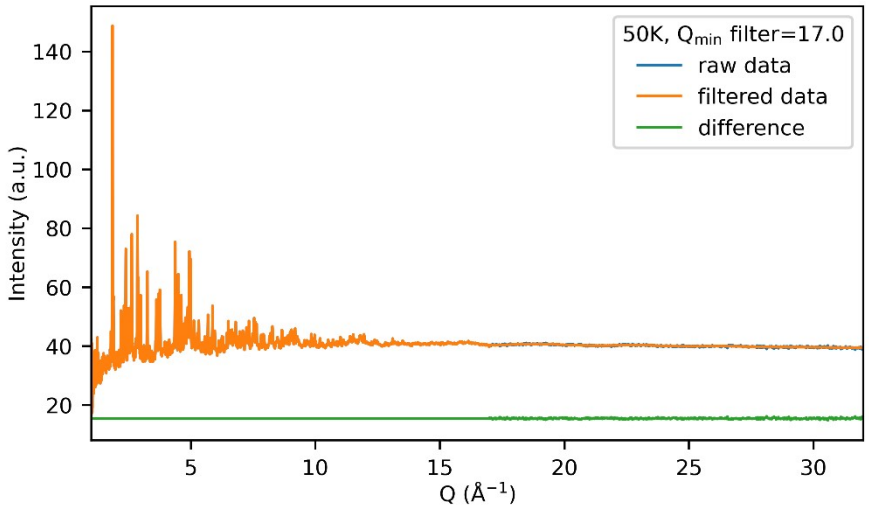

Figure S2: Neutron powder diffraction data collected on $TlTcO_4$ at 50 K on POWGEN at the Spallation Neutron Source at Oak Ridge National Laboratory with the Savitzky-Golay filter applied from $Q \geq 17.0$ Å^{-1}. The blue line represents the collected time of flight data, the orange line represents the filtered data, and the green line shows the difference between the two.

From the collected dataset, the total scattering structure function, $S(Q)$, is calculated by scaling the measured intensity by the compositional average $S(Q) = I(Q)/\langle b \rangle^2$. From this, the reduced structure function $F(Q)$ is derived as $F(Q) = Q[S(Q) - 1]$. The smoothing process was shown to remove the noise in the data at high Q.

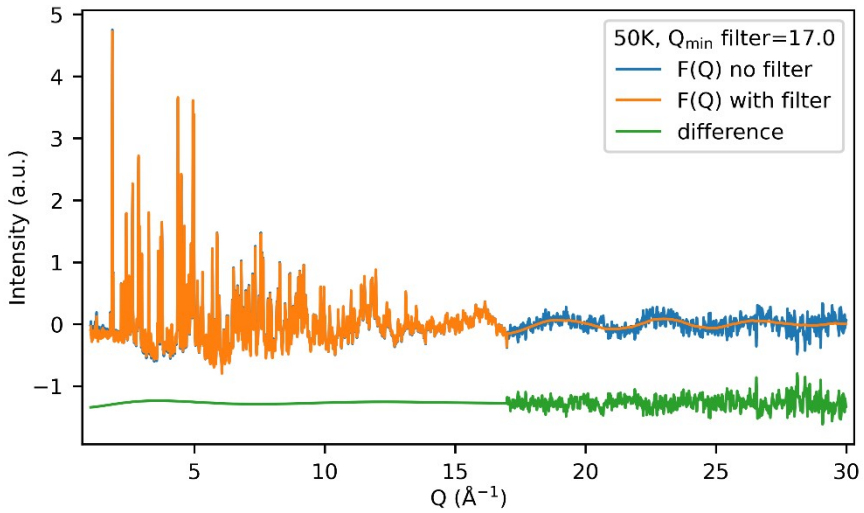

Figure S3: The reduced scattering function, $F(Q)$, of $TlTcO_4$ at 50 K with a Savitzky-Golay filter applied from $Q \geq 17.0$ Å^{-1}. The blue line represents the data, the orange line represents the filtered data, and the green line shows the difference between the two.

The reduced PDF, $G(r)$, and the reduced structure function, $F(Q)$, are related by the sine Fourier transform. This gives a direct relationship between the experimentally measured pattern and the PDF by $G(r) = \frac{2}{\pi}\int_{Q_{min}}^{Q_{max}} F(Q)\sin(Qr)dQ$, where Q_{max} and Q_{max} are set by the instrument and experimental set up. The effect of applying the Savitzky-Golay filter is evident.

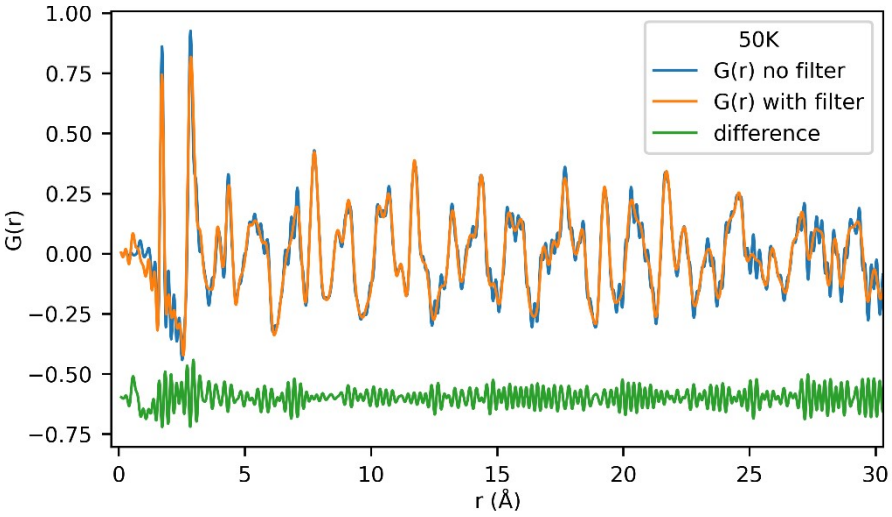

Figure S4: The reduced neutron pair distribution function, $G(r)$, of $TlTcO_4$ at 50 K with a Savitzky-Golay filter applied from $Q \geq$ 17.0 Å^{-1}. The blue line represents the data, the orange line represents the filtered data, and the green line shows the difference between the two.

For the 300 K dataset, the Savitzky-Golay filter was applied to $Q \geq 11.5$ Å^{-1}.

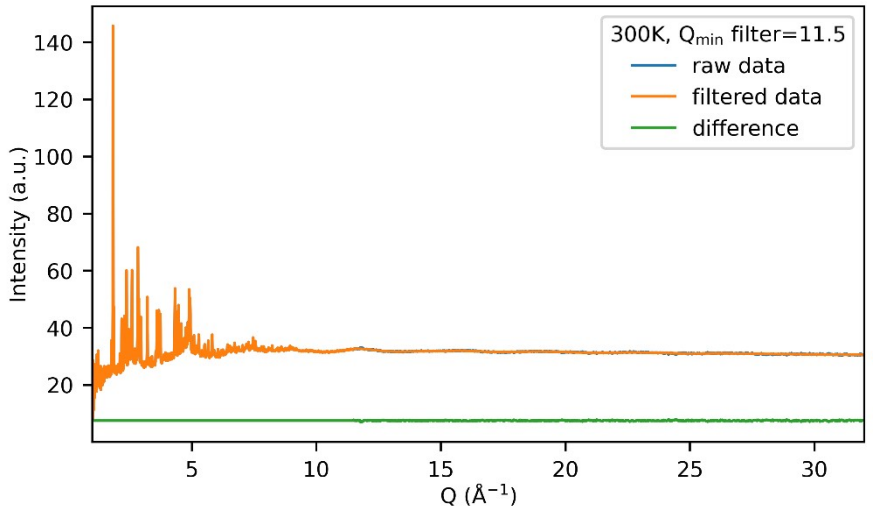

Figure S5: Neutron powder diffraction data collected on $TlTcO_4$ at 300 K on POWGEN at the Spallation Neutron Source at Oak Ridge National Laboratory with the Savitzky-Golay filter applied from $Q \geq 11.5$ Å^{-1}. The blue line represents the collected time of flight data, the orange line represents the filtered data, and the green line shows the difference between the two.

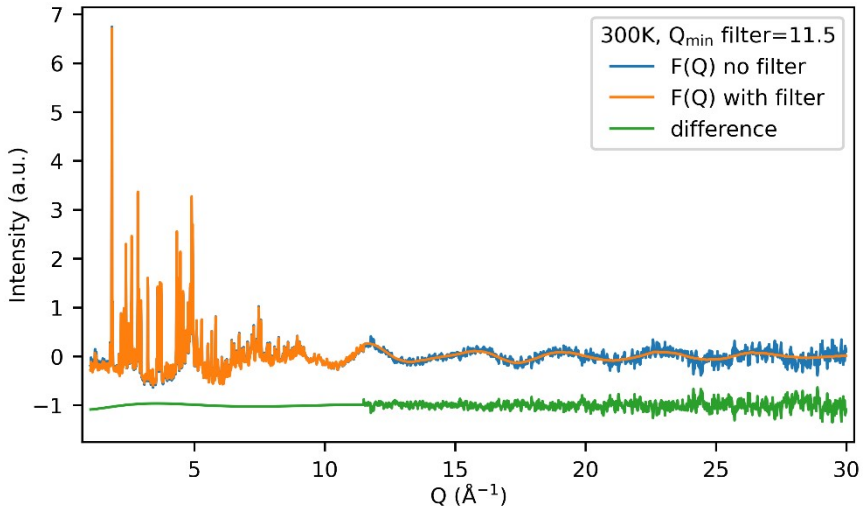

Figure S6: The reduced scattering function, $F(Q)$, of $TlTcO_4$ at 300 K with a Savitzky-Golay filter applied from $Q \geq 11.5$ Å^{-1}. The blue line represents the data, the orange line represents the filtered data, and the green line shows the difference between the two.

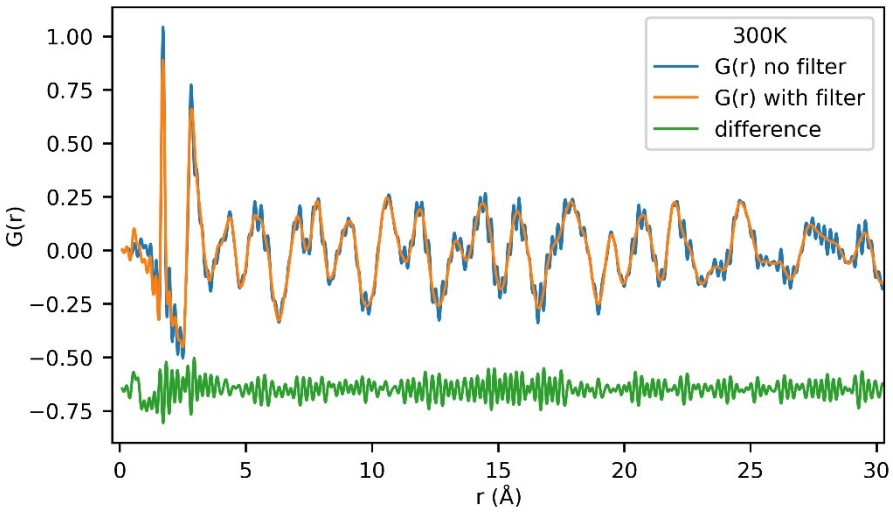

Figure S7: The reduced neutron pair distribution function, $G(r)$, of $TlTcO_4$ at 300 K with a Savitzky-Golay filter applied from $Q \geq 11.5$ Å^{-1}. The blue line represents the data, the orange line represents the filtered data, and the green line shows the difference between the two.

For the 450 K dataset, the Savitzky-Golay filter was applied to $Q \geq 10.5$ Å^{-1}.

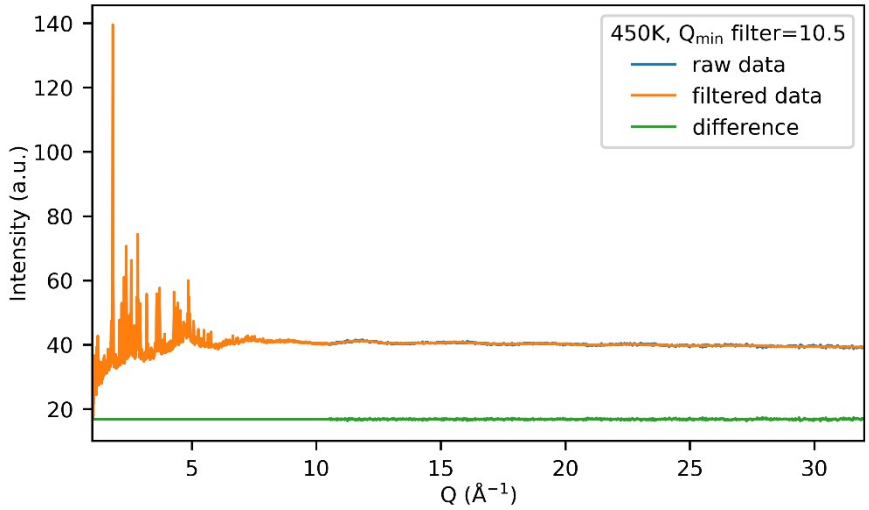

Figure S8: Neutron powder diffraction data collected on $TlTcO_4$ at 450 K on POWGEN at the Spallation Neutron Source at Oak Ridge National Laboratory with the Savitzky-Golay filter applied from $Q \geq 10.5$ Å^{-1}. The blue line represents the collected time of flight data, the orange line represents the filtered data, and the green line shows the difference between the two.

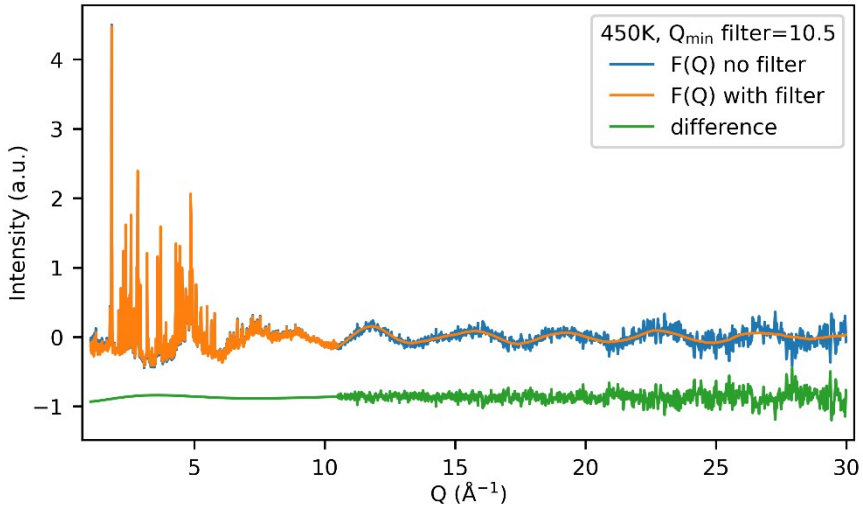

Figure S9: The reduced scattering function, $F(Q)$, of $TlTcO_4$ at 300 K with a Savitzky-Golay filter applied from $Q \geq 10.5$ Å^{-1}. The blue line represents the data, the orange line represents the filtered data, and the green line shows the difference between the two.

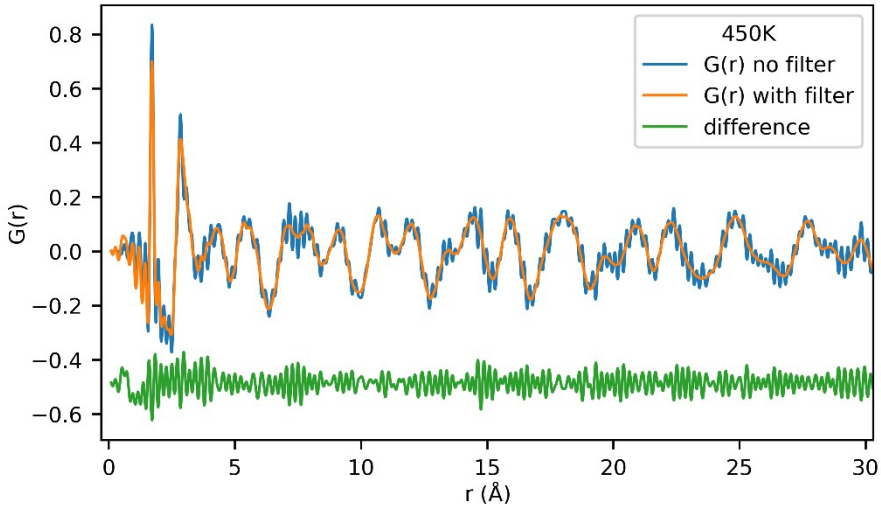

Figure S10: The reduced neutron pair distribution function, $G(r)$, of $TlTcO_4$ at 450 K with a Savitzky-Golay filter applied from $Q \geq 10.5$ Å^{-1}. The blue line represents the data, the orange line represents the filtered data, and the green line shows the difference between the two.

For the 600 K dataset, the Savitzky-Golay filter was applied to $Q \geq 9.0$ Å^{-1}.

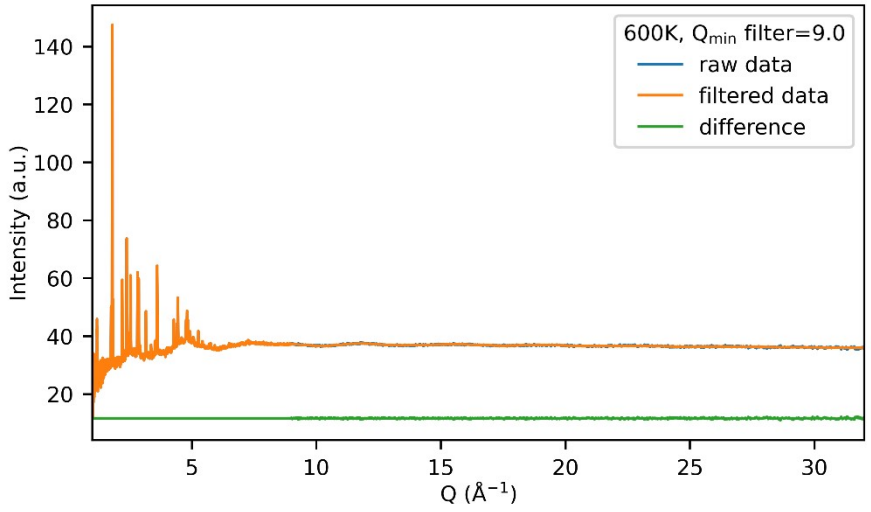

Figure S11: Neutron powder diffraction data collected on $TlTcO_4$ at 600 K on POWGEN at the Spallation Neutron Source at Oak Ridge National Laboratory with the Savitzky-Golay filter applied from $Q \geq 9.0$ Å^{-1}. The blue line represents the collected time of flight data, the orange line represents the filtered data, and the green line shows the difference between the two.

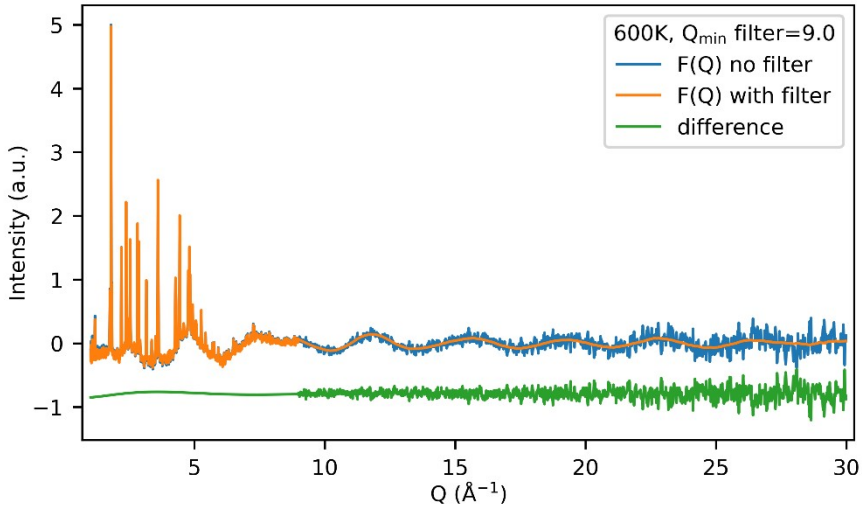

Figure S12: The reduced scattering function, $F(Q)$, of $TlTcO_4$ at 600 K with a Savitzky-Golay filter applied from $Q \geq 9.0$ Å^{-1}. The blue line represents the data, the orange line represents the filtered data, and the green line shows the difference between the two.

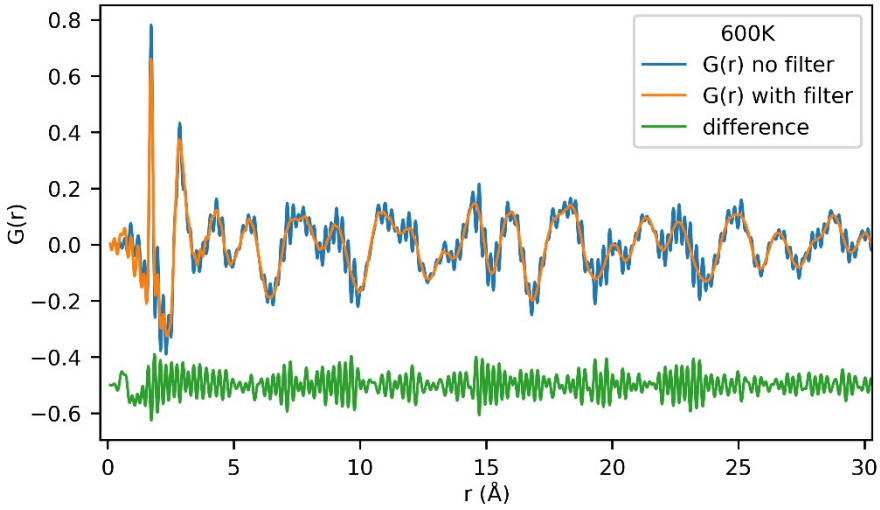

Figure S13: The reduced neutron pair distribution function, $G(r)$, of $TlTcO_4$ at 600 K with a Savitzky-Golay filter applied from $Q \geq 9.0$ Å^{-1}. The blue line represents the data, the orange line represents the filtered data, and the green line shows the difference between the two.

(i) *Neutron Powder Diffraction and Rietveld Analysis*

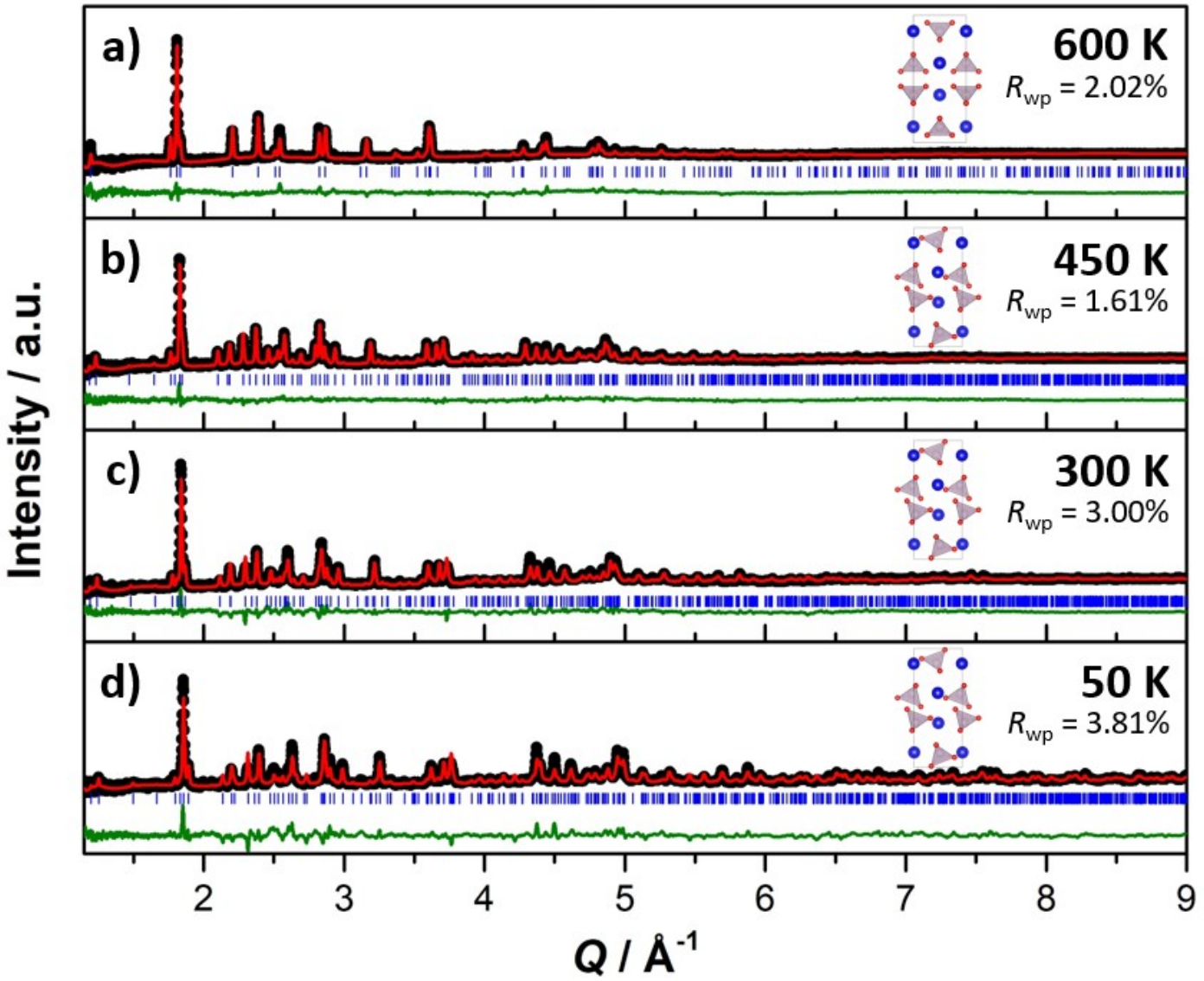

Figure S14: Rietveld refinements to the neutron Bragg data of $TlTcO_4$ at (a) 600 K to the tetragonal $I4_1/amd$ space group, (b) 450 K to the orthorhombic *Pnma* space group, (c) 300 K to the orthorhombic *Pnma* space group, and (d) 50 K to the orthorhombic *Pnma* space group. The black circles represent the collected data, the red line represents the fit to the data, the green line represents the difference between the two, and the blue dashes represent the space group-allowed reflections.

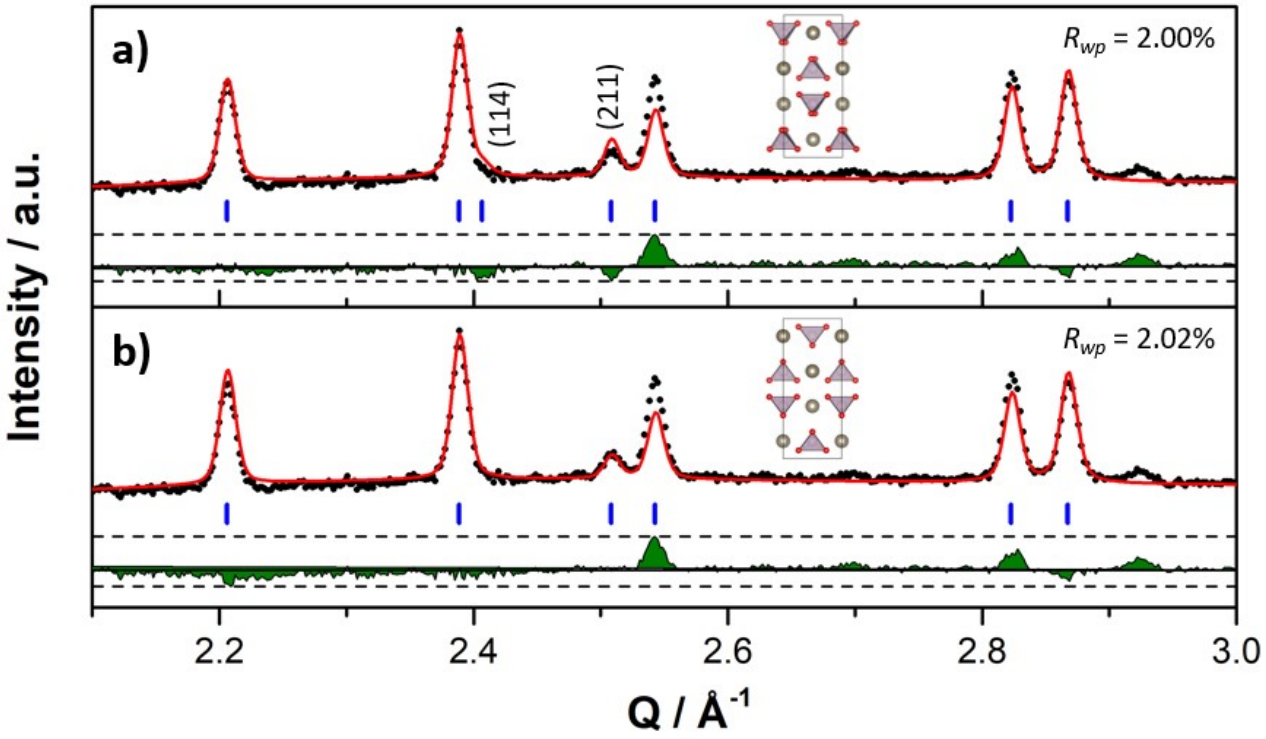

Figure S15: Neutron diffraction pattern of $TlTcO_4$ at 600 K fitted to (a) the tetragonal $I4_1/a$ scheelite-type space group, and (b) the tetragonal $I4_1/amd$ scheelite-type aristotype space group. The black circles represent the diffraction data, the red line is the Rietveld refinement, the green is the difference between the two, and the blue lines are the space group-allowed reflections of each phase. The (114) reflection are allowed in the $I4_1/a$ but forbidden in the $I4_1/amd$ structure.

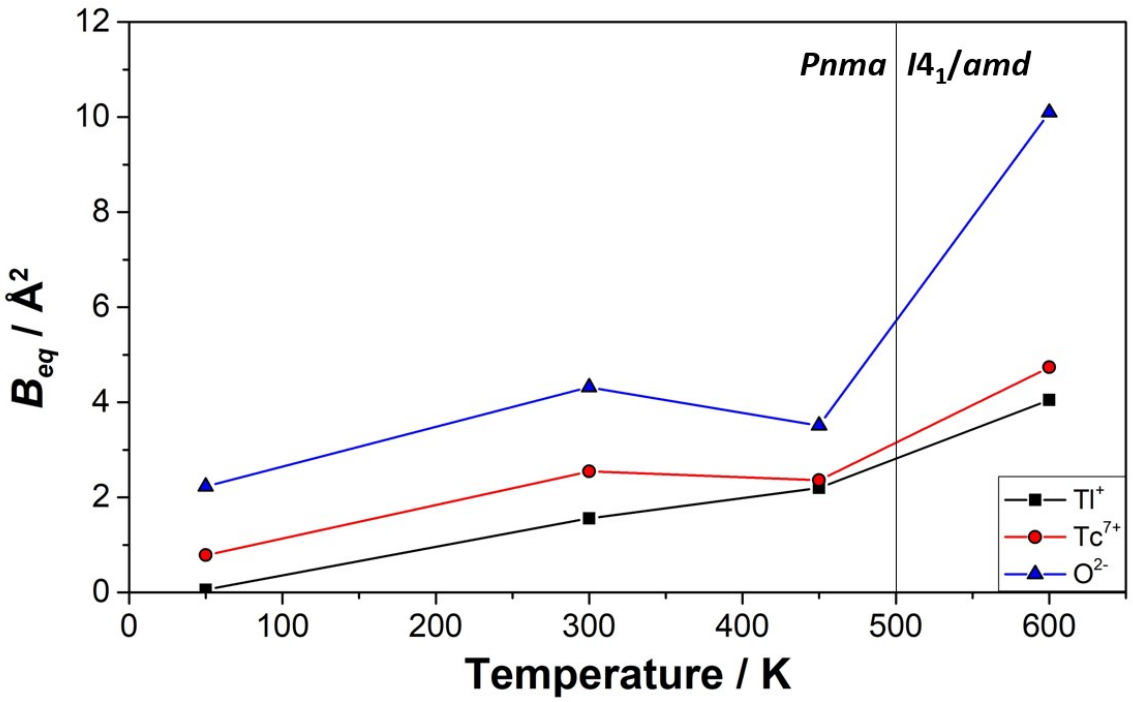

Figure S16: Refined atomic displacement parameters of the atoms in $TlTcO_4$, taken from the Rietveld refinements on the POWGEN neutron diffraction data. The solid line indicates the orthorhombic *Pnma* to tetragonal $I4_1/amd$ phase transition.

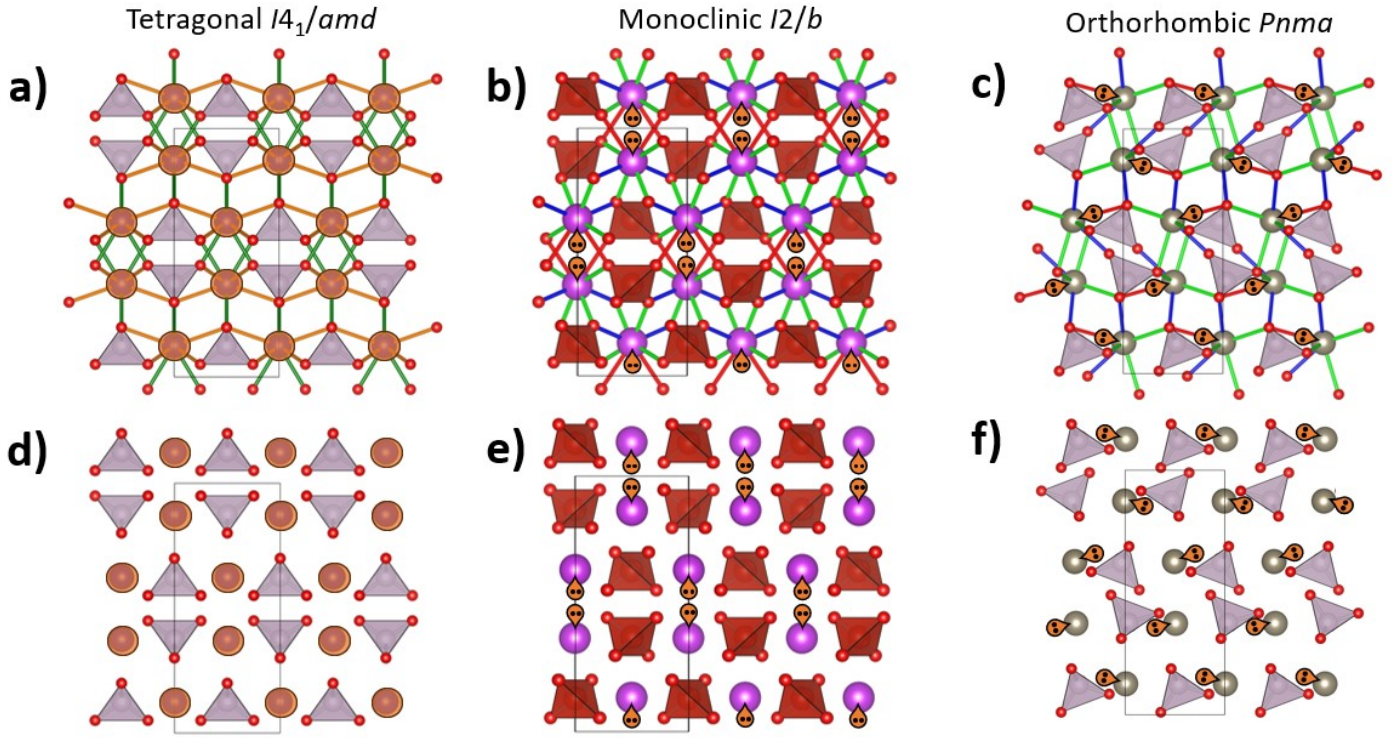

Figure S17: Crystallographic models for (a,d) $TlTcO_4$ $I4_1/amd$ (SG #141), (b,e) $BiVO_4$ $I2/b$ (#15), and (c,f) $TlTcO_4$ $Pnma$ (SG #62). The top row (a-c) shows the structure with various A-O bond lengths color-coded in terms of length (blue is short, green and orange is medium, and red is long). The bottom row (d-f) shows the structure with the BO_4 tetrahedra drawn and the lone pairs drawn in orange.

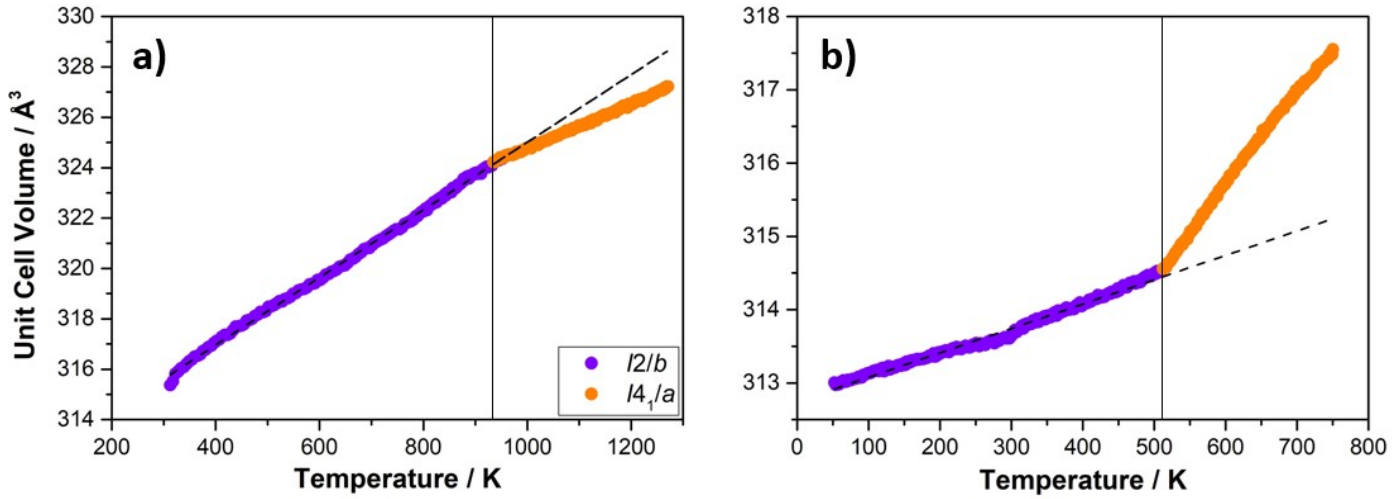

Figure S18: Variable temperature unit cell volume of (a) $NdNbO_4$ ($6s^0$) and (b) $BiVO_4$ ($6s^2$). The solid line indicates the monoclinic $I2/b$ to tetragonal $I4_1/a$ phase transition, and the dashed line has been drawn to guide the eyes.

Table S1: Rietveld refinement structural parameters for $TlTcO_4$ using neutron powder diffraction data collected on POWGEN at Oak Ridge National Laboratory.

Temperature (K)		**50**	**300**	**450**	**600**
Space Group		*Pnma*	*Pnma*	*Pnma*	$I4_1/amd$
***a* (Å)**		5.4381(7)	5.4867(8)	5.5221(7)	5.7112(8)
***b* (Å)**		5.7252(6)	5.7576(8)	5.7653(7)	= *a*
***c* (Å)**		13.3167(16)	13.4977(19)	13.6391(18)	13.746
Volume (Å^3)		414.60(8)	426.40(10)	434.22(10)	448.37(15)
Tl	***x***	0.0057(11)	0.0136(13)	0.0269(11)	= 0
	y	= 3/4	= 3/4	= 3/4	= 3/4
	z	0.1264(5)	0.1261(5)	0.1269(4)	= 1/8
Tc	***x***	0.0347(15)	0.0312(17)	0.0353(13)	= 0
	y	= 1/4	= 1/4	= 1/4	= 1/4
	z	0.3769(8)	0.3795(8)	0.3804(5)	= 3/8
O(1)	***x***	0.840(3)	0.820(3)	0.8285(17)	= 0
	y	= 1/4	= 1/4	= 1/4	0.5128(15)
	z	0.0849(10)	0.0809(9)	0.0826(6)	0.6910(5)
O(2)	***x***	0.858(2)	0.840(3)	0.8479(14)	--
	y	= 1/4	= 1/4	= 1/4	--
	z	0.4896(10)	0.4772(12)	0.4783(7)	--
O(3)	***x***	0.0387(15)	0.0348(14)	0.0250(14)	--
	y	0.5041(13)	0.5035(12)	0.5053(10)	--
	z	0.6883(6)	0.6893(5)	0.6889(4)	--
B_{eq} **(Tl) (Å^2)**		0.00(11)	1.41(17)	2.3(2)	3.6(4)
B_{eq} **(Re) (Å^2)**		0.73(17)	2.3(2)	2.3(2)	4.0(4)
B_{eq} **(O) (Å^2)**		2.1(2)	4.2(3)	3.66(18)	10.9(4)

(ii) *Neutron Total Scattering and Pair Distribution Function Analysis*

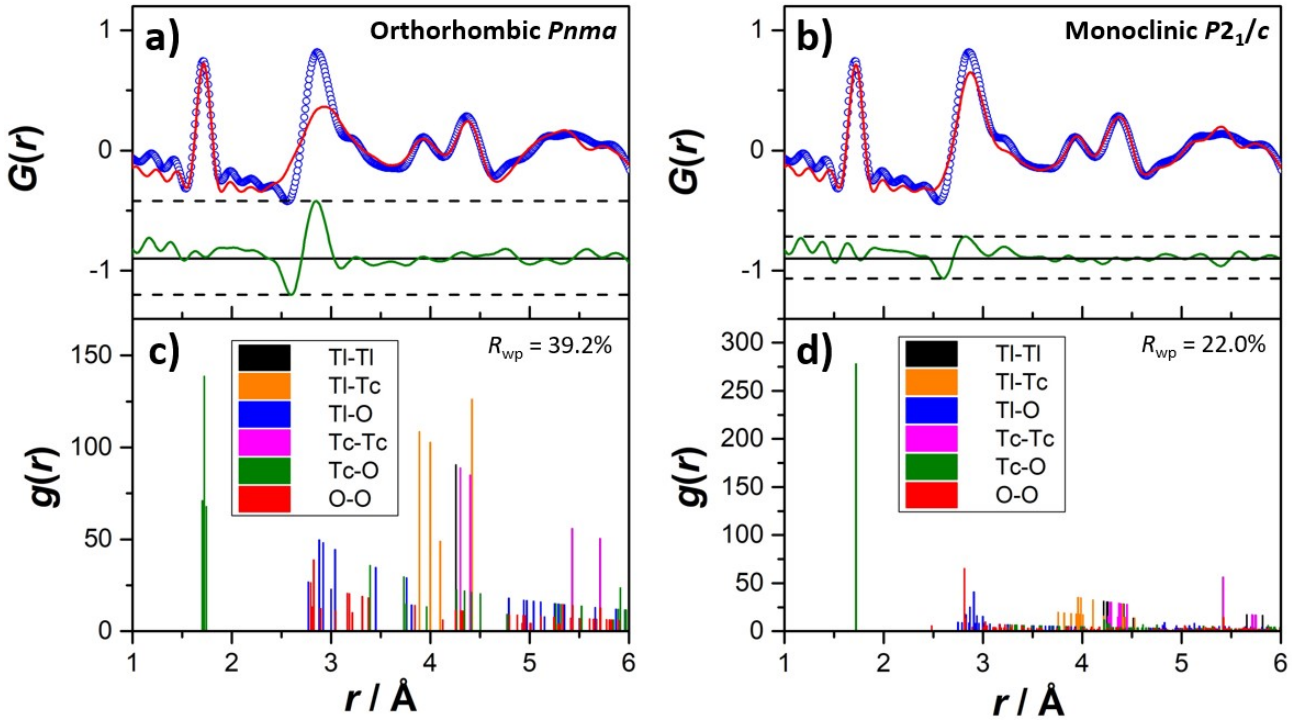

Figure S19: Neutron pair distribution function data of $TlTcO_4$ at 50 K fitted to the (a) orthorhombic *Pnma* and (b) monoclinic $P2_1/c$ models with rigid TcO_4 tetrahedra. The partial pair distribution functions are shown in (c,d). The blue circles represent the data, the red line represents the fit to the data, and the green line in the difference between the two.

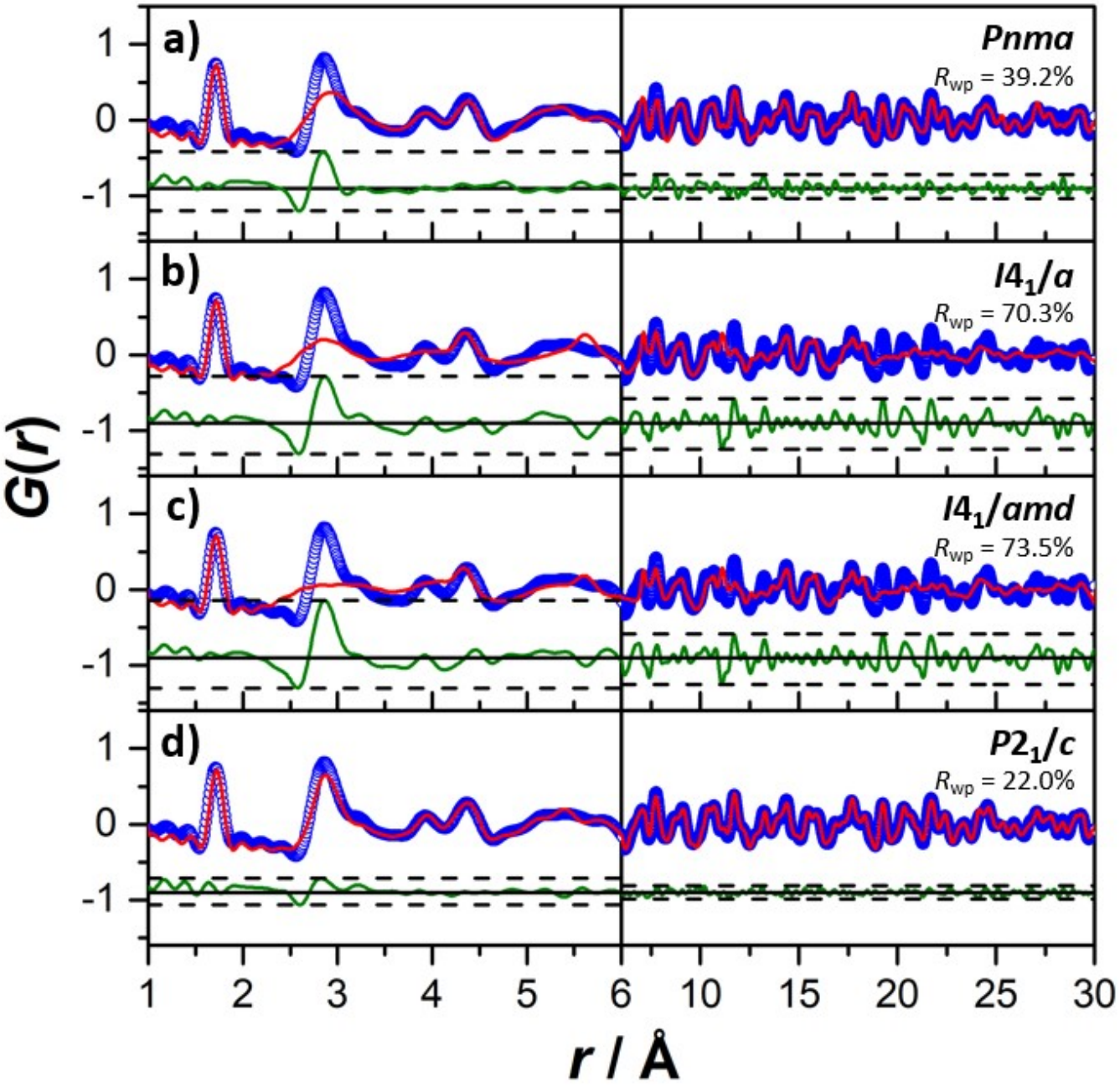

Figure S20: Neutron pair distribution function data of $TlTcO_4$ at 50 K fitted to the (a) orthorhombic *Pnma*, (b) tetragonal $I4_1/a$, (c) tetragonal $I4_1/amd$, and (d) monoclinic $P2_1/c$. In each of the fits, the TcO_4 tetrahedra have been constrained such that Tc-O bond distances and O-Tc-O bond angles are the same. The blue circles represent the data, the red line represents the small box fit to the data, and the green line represents the difference between the two.

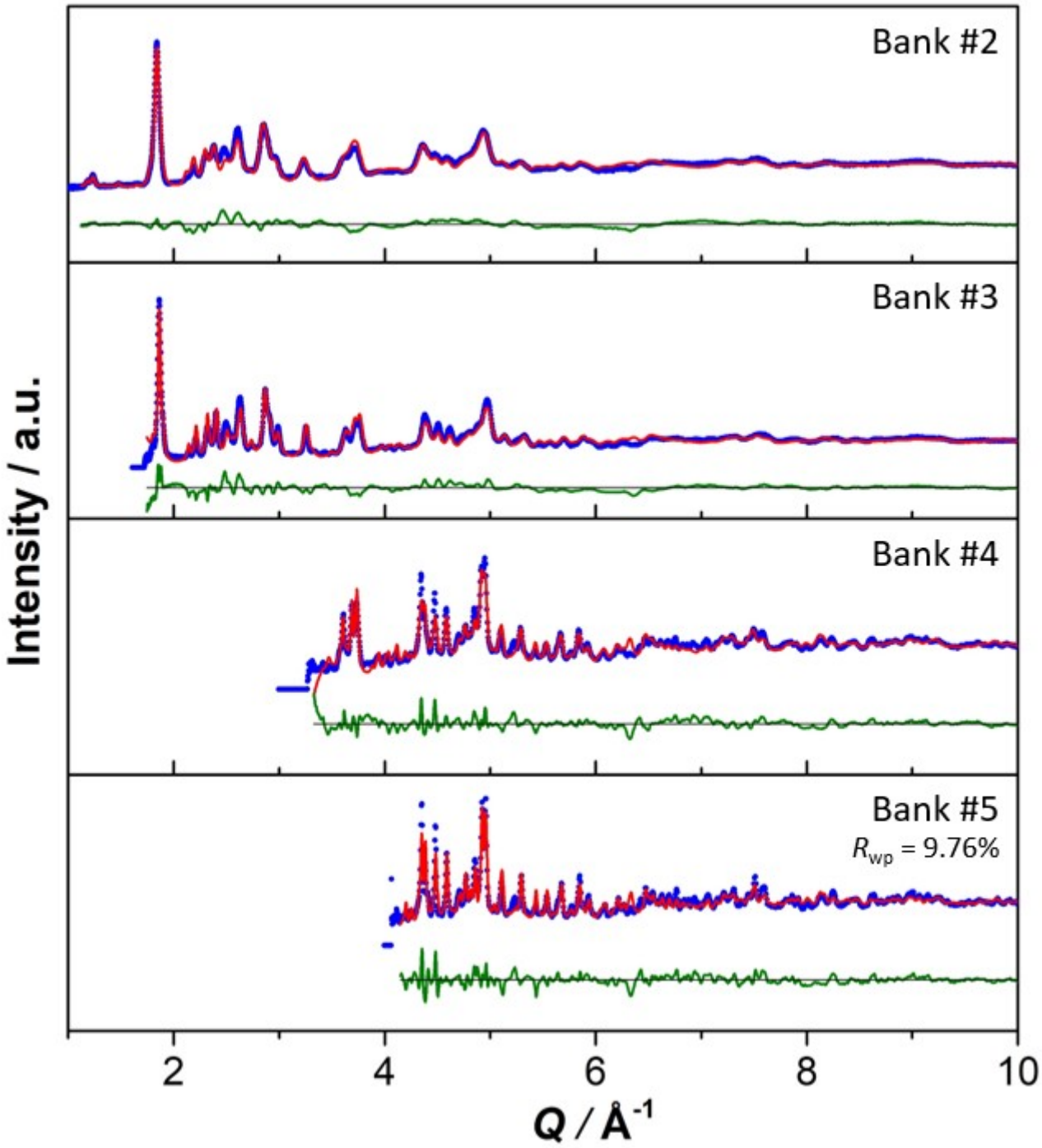

Figure S21: Rietveld refinement of $TlTcO_4$ at 100 K to the orthorhombic *Pnma* model on the NOMAD beamline at Oak Ridge National Laboratory. Data is displayed from the four highest resolution detector banks. The blue circles represent the data, the solid red line is the fit to the data, and the solid green line is the difference between the two.

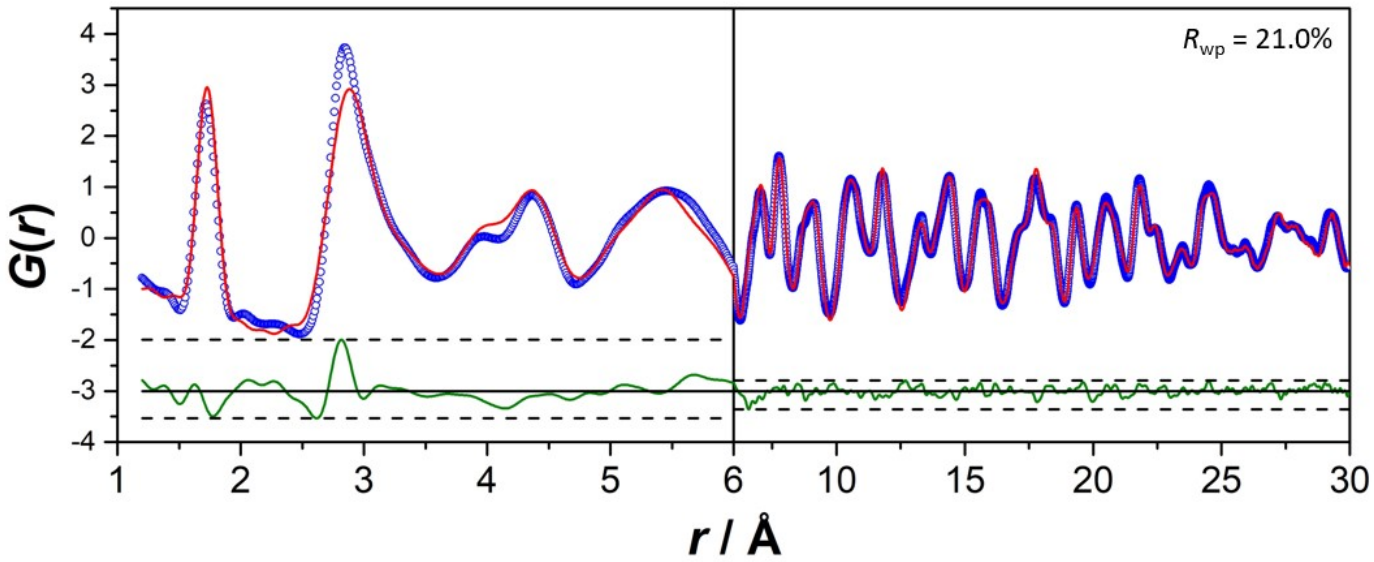

Figure S22: Neutron pair distribution function data for $TlTcO_4$ using data collected on the NOMAD beamline at Oak Ridge National Laboratory. Data has been Fourier transformed with the Lorch function to aid in smoothing out the peaks. The blue circles represent the data, the solid red line is the fit to the data, and the solid green line is the difference between the two. The dashed lines indicate the maximum and minimum in the difference curve across the plotted *r* ranges.

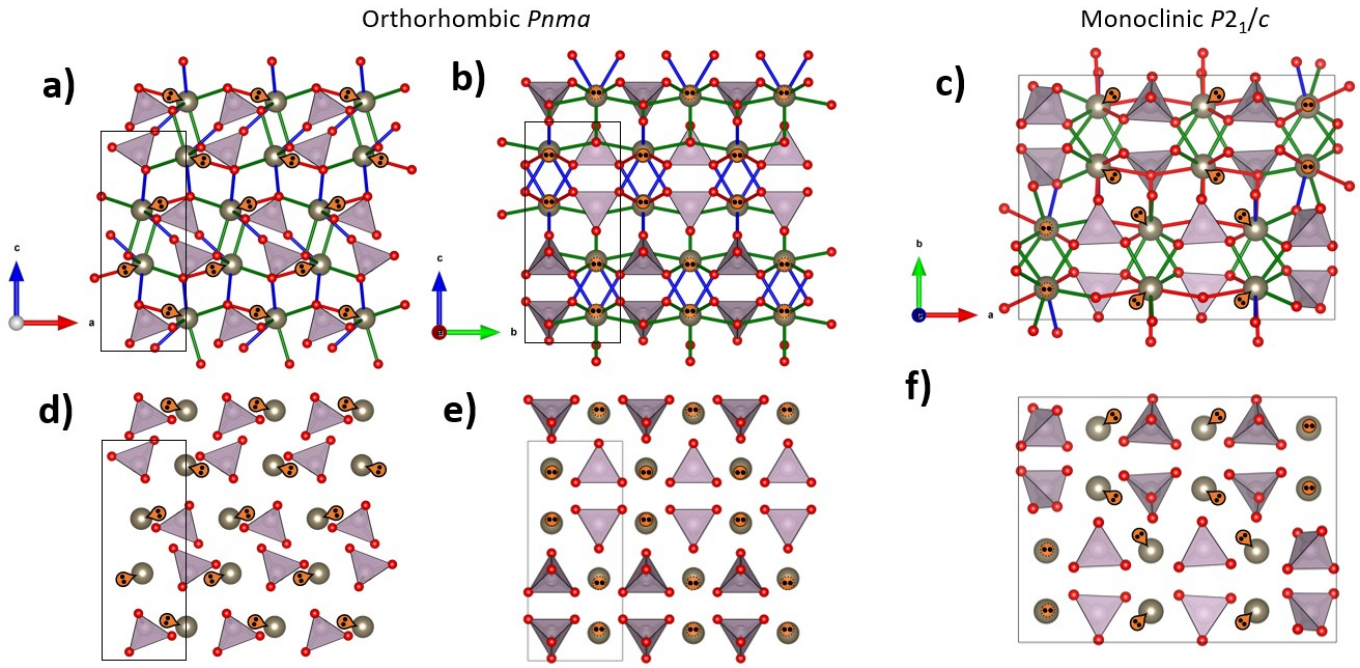

Figure S23: Crystallographic models for (a,b,d,e) orthorhombic *Pnma*, (c,f) monoclinic $P2_1/c$. The top row (a-c) shows the structure with various *A*-O bond lengths color-coded in terms of length (blue is short, green and orange is medium, and red is long). The bottom row (d-f) shows the structure with the BO_4 tetrahedra drawn and the lone pairs drawn in orange.

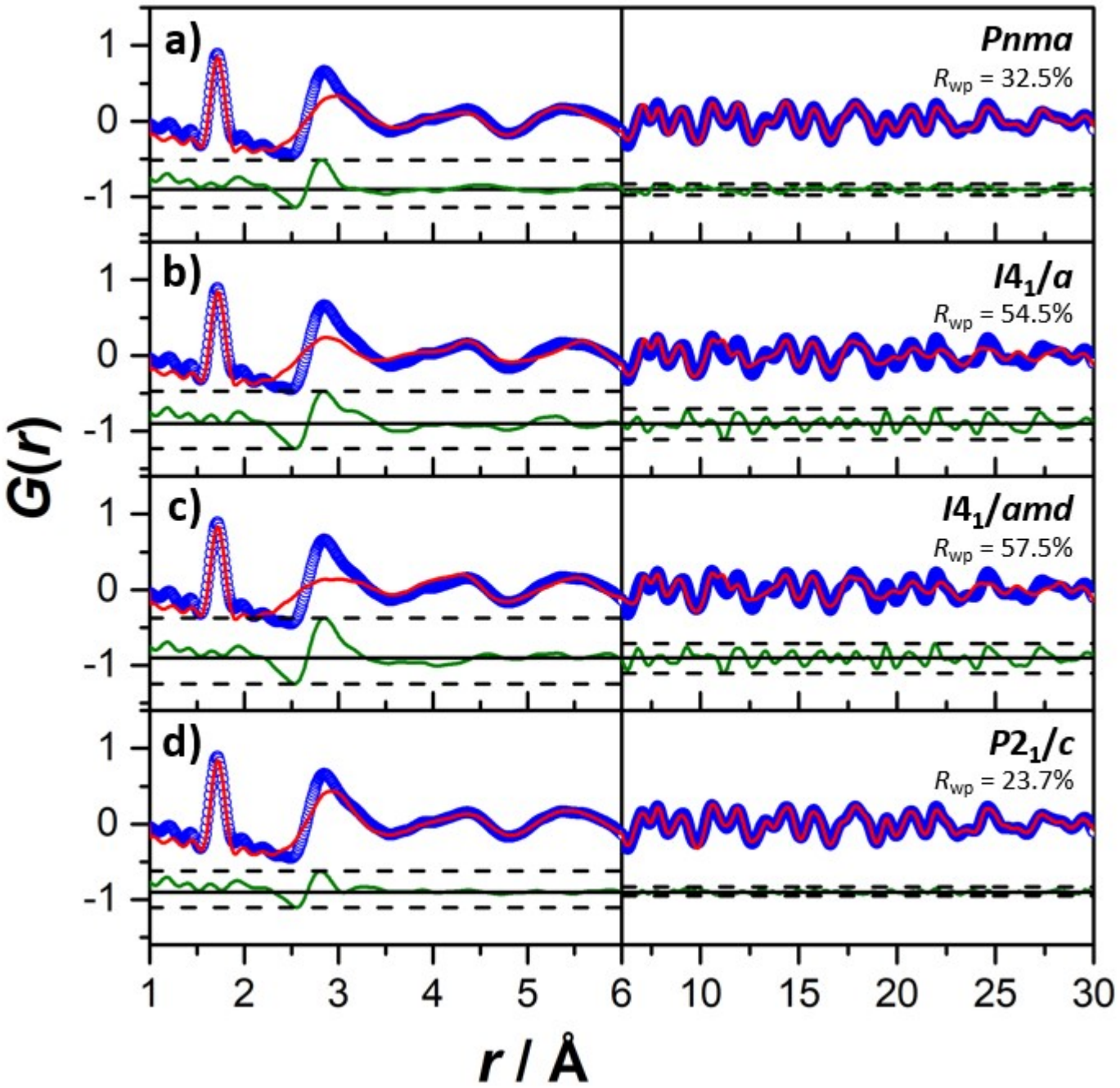

Figure S24: Neutron pair distribution function data of $TlTcO_4$ at 300 K fitted to the (a) orthorhombic *Pnma*, (b) tetragonal $I4_1/a$, (c) tetragonal $I4_1/amd$, and (d) monoclinic $P2_1/c$. In each of the fits, the TcO_4 tetrahedra have been constrained such that Tc-O and O-Tc-O are the same. The blue circles represent the data, the red line represents the small box fit to the data, and the green line represents the difference between the two.

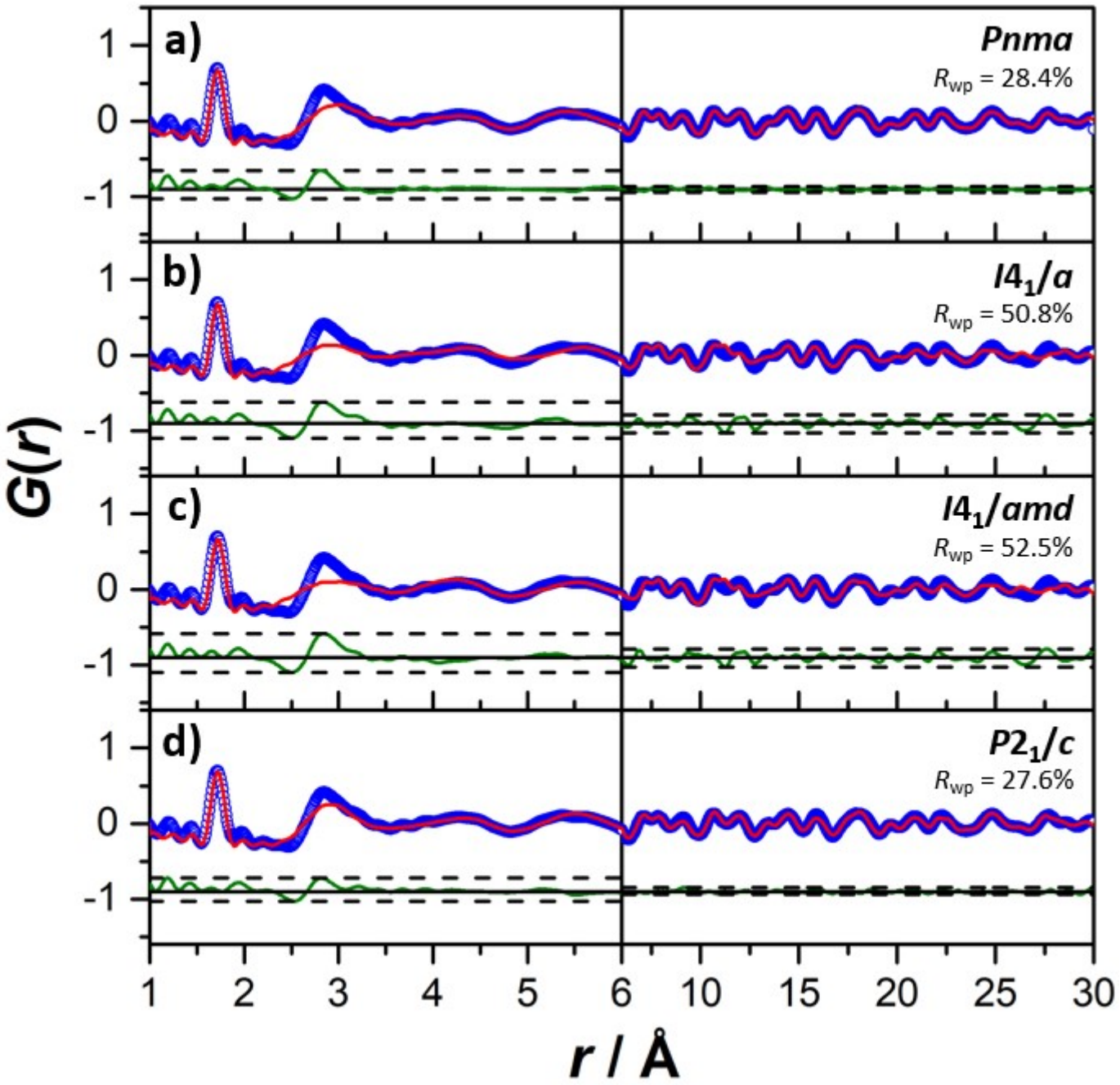

Figure S25: Neutron pair distribution function data of $TlTcO_4$ at 450 K fitted to the (a) orthorhombic *Pnma*, (b) tetragonal $I4_1/a$, (c) tetragonal $I4_1/amd$, and (d) monoclinic $P2_1/c$. In each of the fits, the TcO_4 tetrahedra have been constrained such that Tc-O and O-Tc-O are the same. The blue circles represent the data, the red line represents the small box fit to the data, and the green line represents the difference between the two.

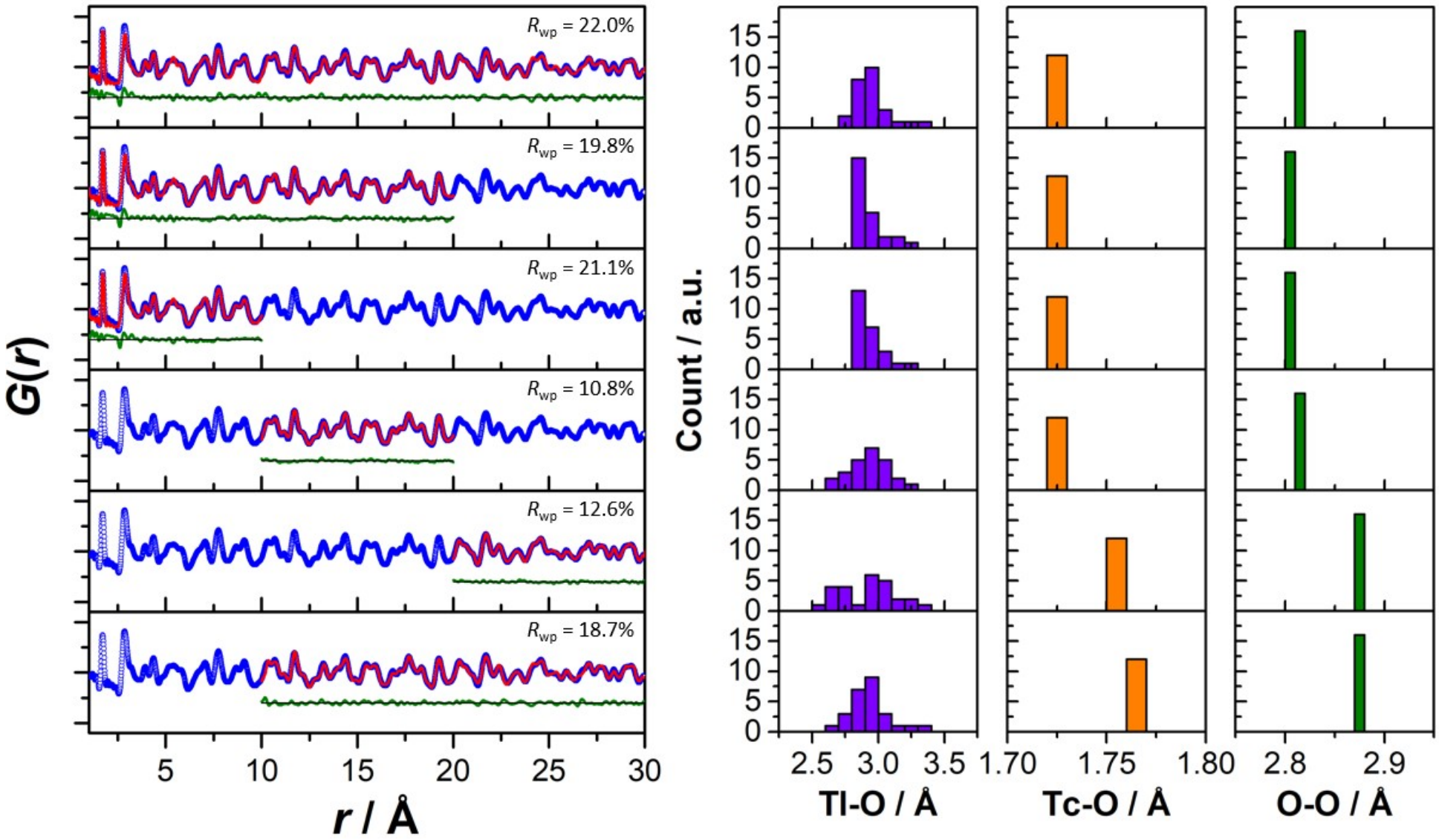

Figure S26: Neutron pair distribution function data of $TlTcO_4$ fitted across different length windows to the monoclinic $P2_1/c$ model. In each of the fits, the TcO_4 tetrahedra have been constrained such that the Tc-O bond distances and O-Tc-O bond angles are the same. The blue circles represent the data, the red line represents the small box fit to the data, and the green line represents the difference between the two. The histograms on the right show the range of Tl-O and Tc-O bond distances, as well as the O-O distances across the TcO_4 tetrahedra across each fit.

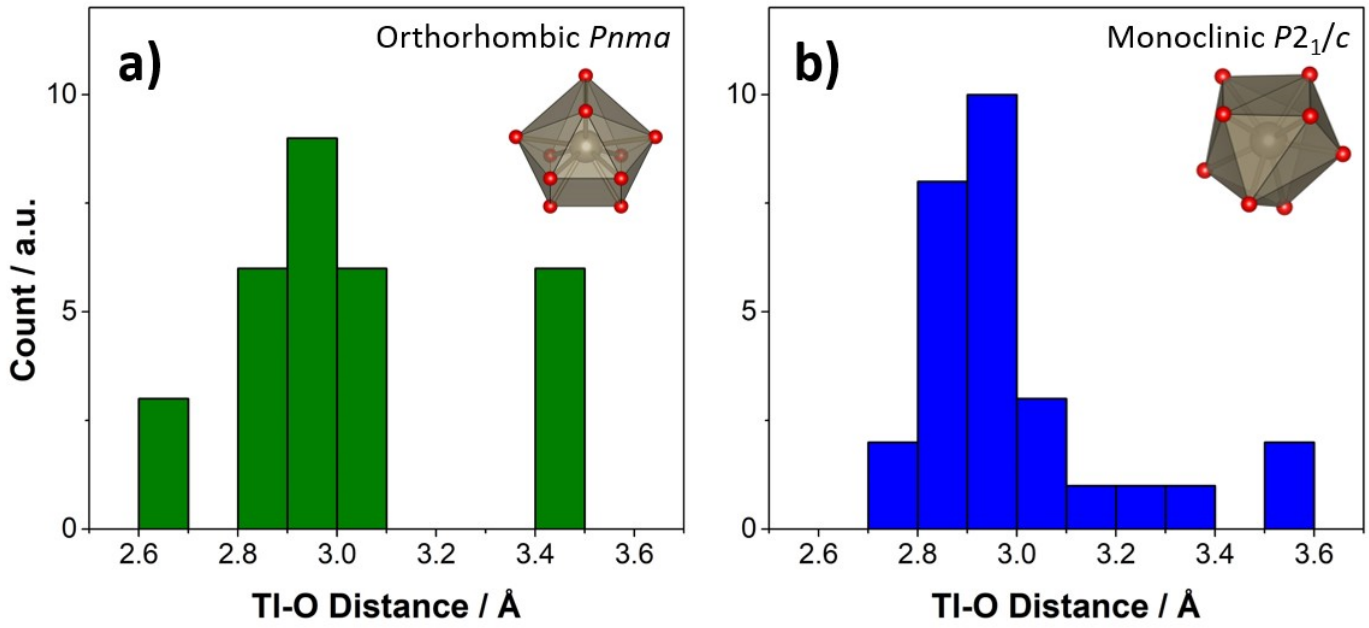

Figure S27: Distribution of Tl-O bond distances in the Tl polyhedra of $TlTcO_4$ at 50 K extracted from (a) the Rietveld refinement of the neutron powder diffraction data fit to the orthorhombic *Pnma* model, and (b) the small box fit of the neutron pair distribution function to the monoclinic $P2_1/c$ model with rigid TcO_4 tetrahedra.

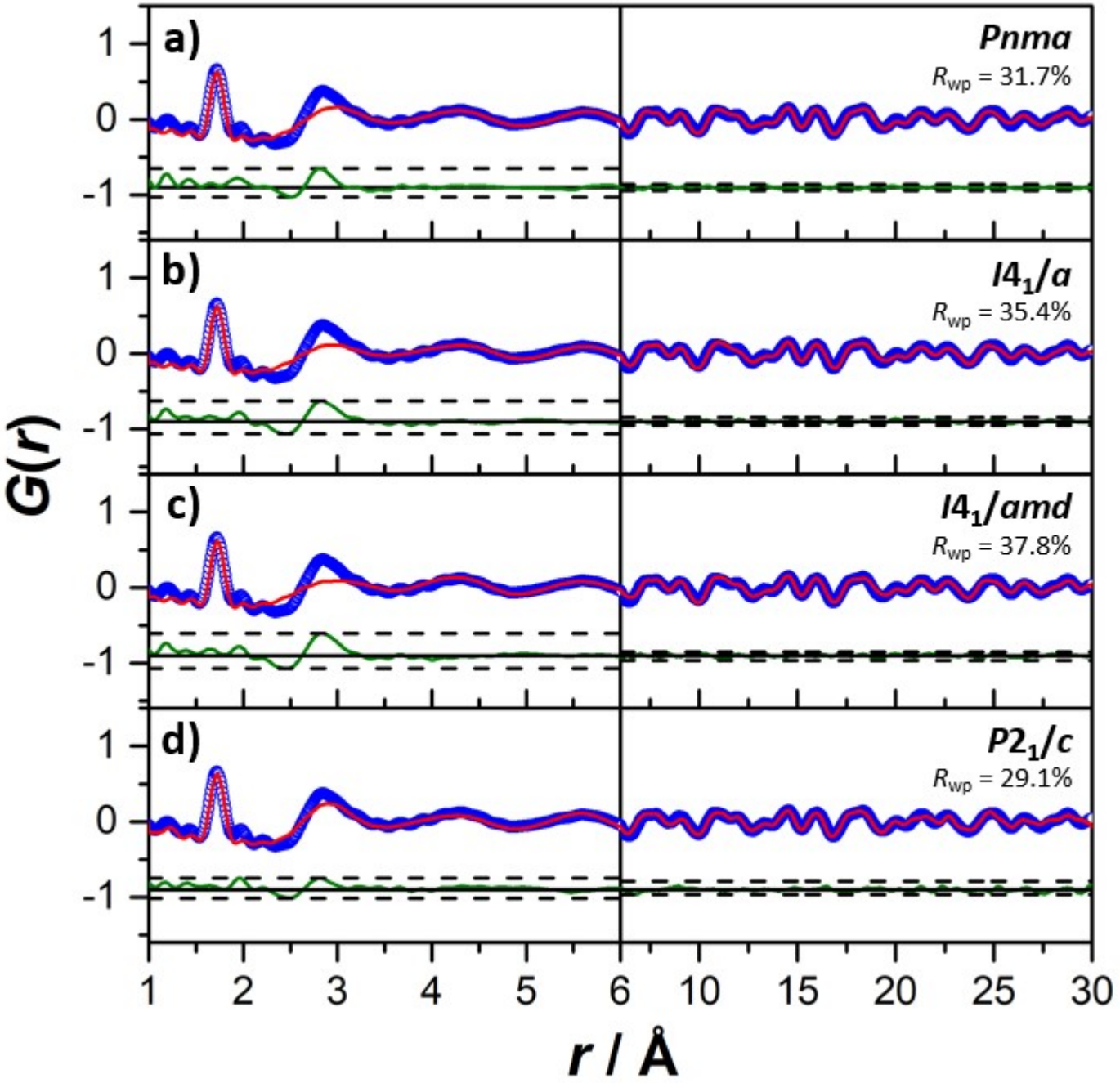

Figure S28: Neutron pair distribution function data of $TlTcO_4$ at 600 K fitted to the (a) orthorhombic *Pnma*, (b) tetragonal $I4_1/a$, (c) tetragonal $I4_1/amd$, and (d) monoclinic $P2_1/c$. In each of the fits, the TcO_4 tetrahedra have been constrained such that Tc-O and O-Tc-O are the same. The blue circles represent the data, the red line represents the small box fit to the data, and the green line represents the difference between the two.

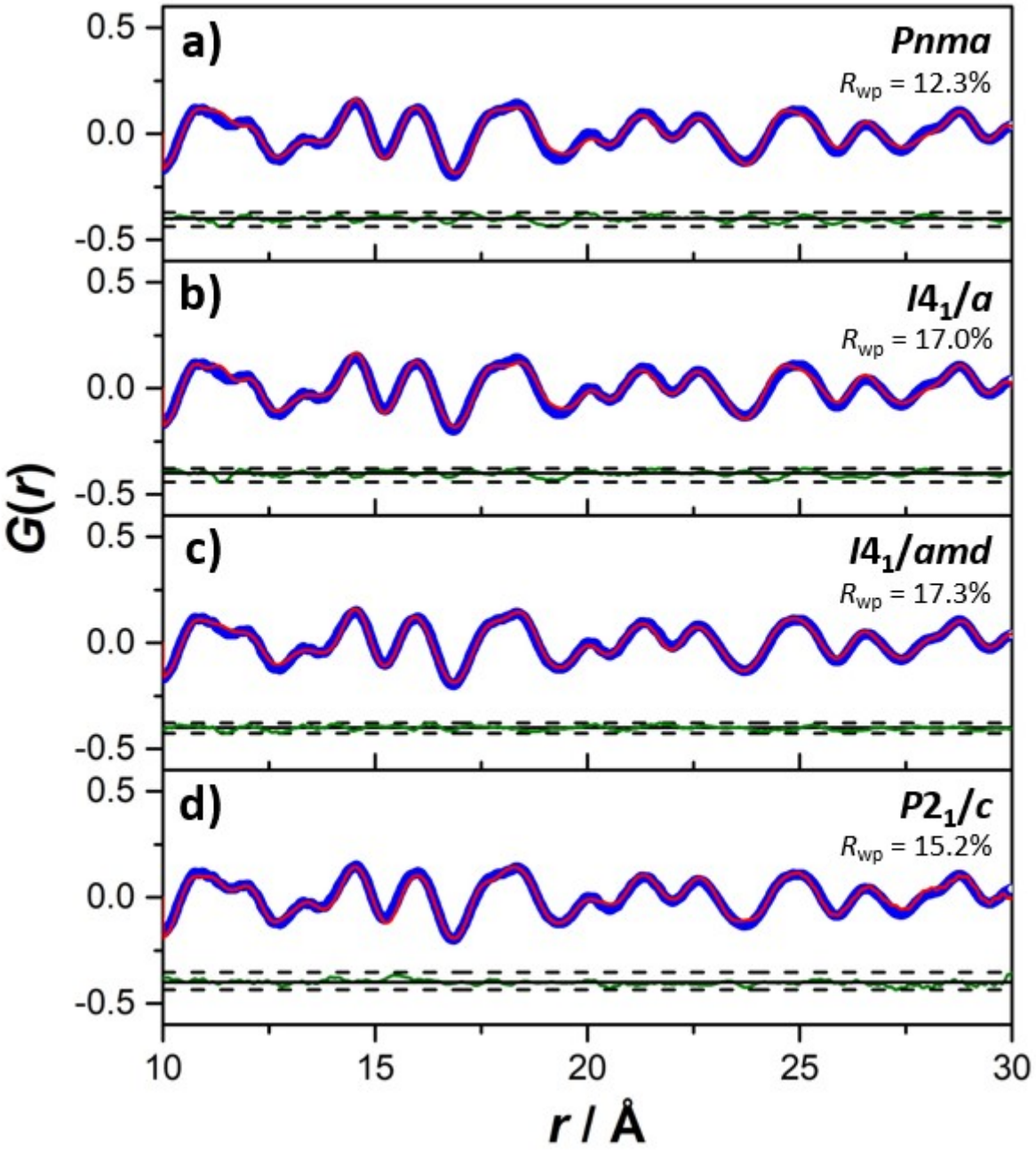

Figure S29: Neutron pair distribution function data of $TlTcO_4$ at 600 K fitted to the (a) orthorhombic *Pnma*, (b) tetragonal $I4_1/a$, (c) tetragonal $I4_1/amd$, and (d) monoclinic $P2_1/c$, fitted over the range of 10-30 Å. In each of the fits, the TcO_4 tetrahedra have been constrained such that Tc-O and O-Tc-O are the same. The blue circles represent the data, the red line represents the small box fit to the data, and the green line represents the difference between the two.

(iii) Ground State Energy Calculations Using Density-Functional Theory

Table S2: Density functional theory calculations for $TlTcO_4$ calculated using the structures modelled from the neutron pair distribution function data collected at 50 K.

			AM05		PBEsol		PBE	
		Exp.	**Calc.**	**Error**	**Calc.**	**Error**	**Calc.**	**Error**
Tetragonal ***I*4$_1$/*a***	***a* (Å)**	5.7116	5.7265	0.26	5.6586	-0.93	5.8062	1.66
	***c* (Å)**	13.7450	13.0206	-5.27	12.6912	-7.67	13.2672	-3.48
	***V* (Å^3)**	448.3945	427.00	-4.77	406.37	-9.37	447.27	-0.25
Tetragonal ***I*4$_1$/*amd***	***a* (Å)**	5.7115	5.8040	1.62	5.6327	-1.38	5.8538	2.49
	***c* (Å)**	13.7460	13.3638	-2.78	13.4062	-2.47	13.5985	-1.07
	***V* (Å^3)**	448.4114	450.20	0.40	425.36	-5.14	465.99	3.92
Orthorhombic ***Pnma***	***a* (Å)**	5.4381	5.5013	1.16	5.3511	-1.60	5.5956	2.90
	***b* (Å)**	5.7252	5.7676	0.74	5.6673	-1.01	5.8511	2.20
	***c* (Å)**	13.3167	13.3352	0.14	13.1168	-1.50	13.5015	1.39
	***V* (Å^3)**	414.6049	423.13	2.06	397.79	-4.06	442.06	6.62
Monoclinic ***P*2$_1$/*c***	***a* (Å)**	17.1870	17.2319	0.26	16.9115	-1.60	17.3803	1.12
	***b* (Å)**	13.3750	13.0001	-2.80	12.9310	-3.32	13.4025	0.21
	***c* (Å)**	5.4528	5.7257	5.00	5.5051	0.96	5.7369	5.21
	***V* (Å^3)**	1253.43	1282.70	2.34	1203.76	-3.96	1336.31	6.61

Table S3: Ground state energy calculations using density functional theory for $TlTcO_4$

Structure	**AM05**	**PBEsol**	**PBE**
Tetragonal *I*4$_1$/*a*	-167.8057	-171.9275	-164.2912
Tetragonal *I*4$_1$/*amd*	-167.1769	-171.1409	-1637378
Orthorhombic *Pnma*	-167.4337	-171.6052	-163.9406
Monoclinic *P*2$_1$/*c*	-167.7634	-171.8282	-164.1518

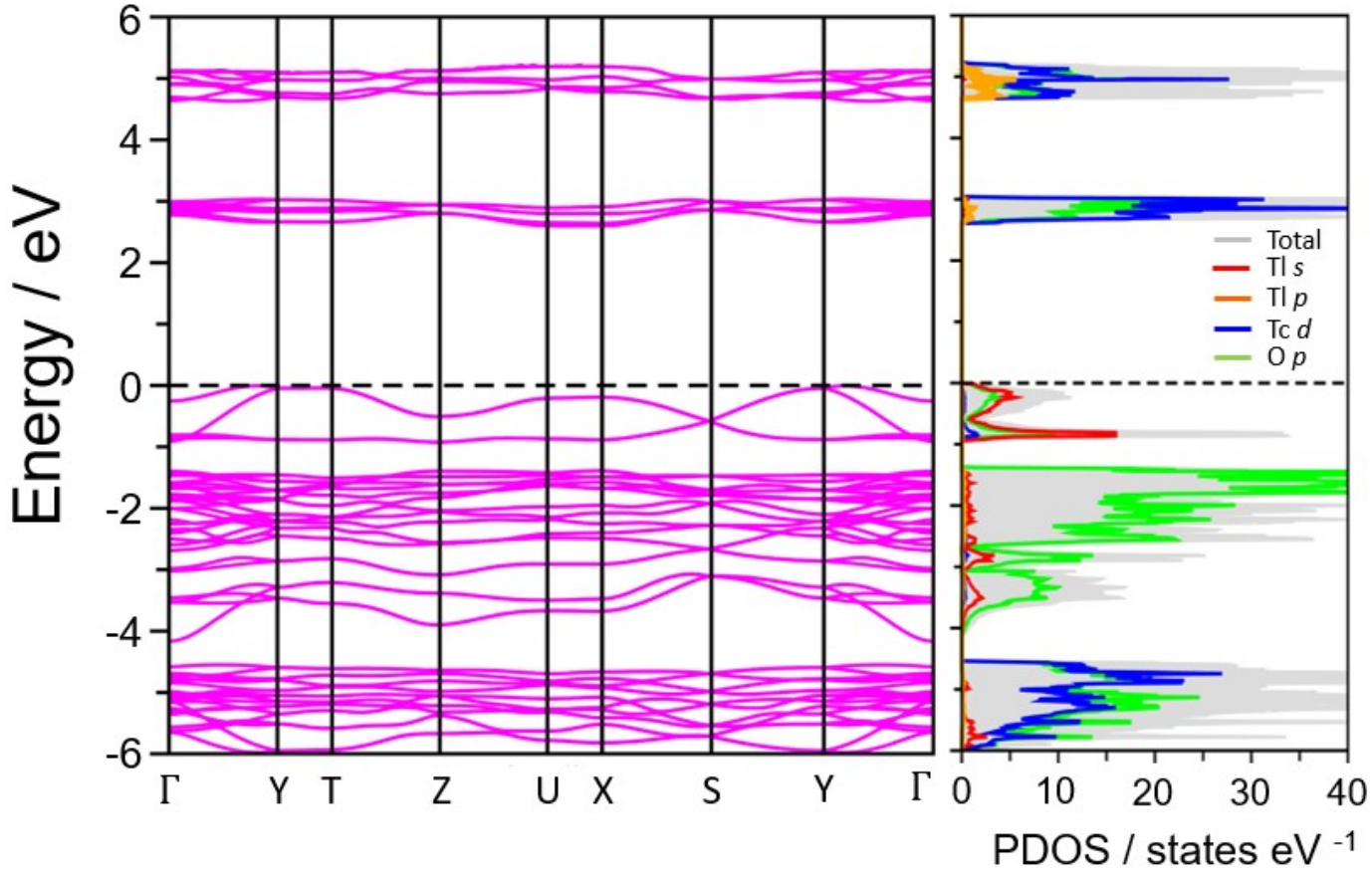

Figure S30: Electronic band structure and partial density of states (PDOS) of $TlTcO_4$ in the orthorhombic *Pnma* space group, calculated using the Tran-Blaha modified Becke-Johnson (TB-mBJ) potential and showing a bandgap of 2.58 eV.

(iv) Comparison Between ABO_4 Structures with $6s^2$ Lone Pair Electrons

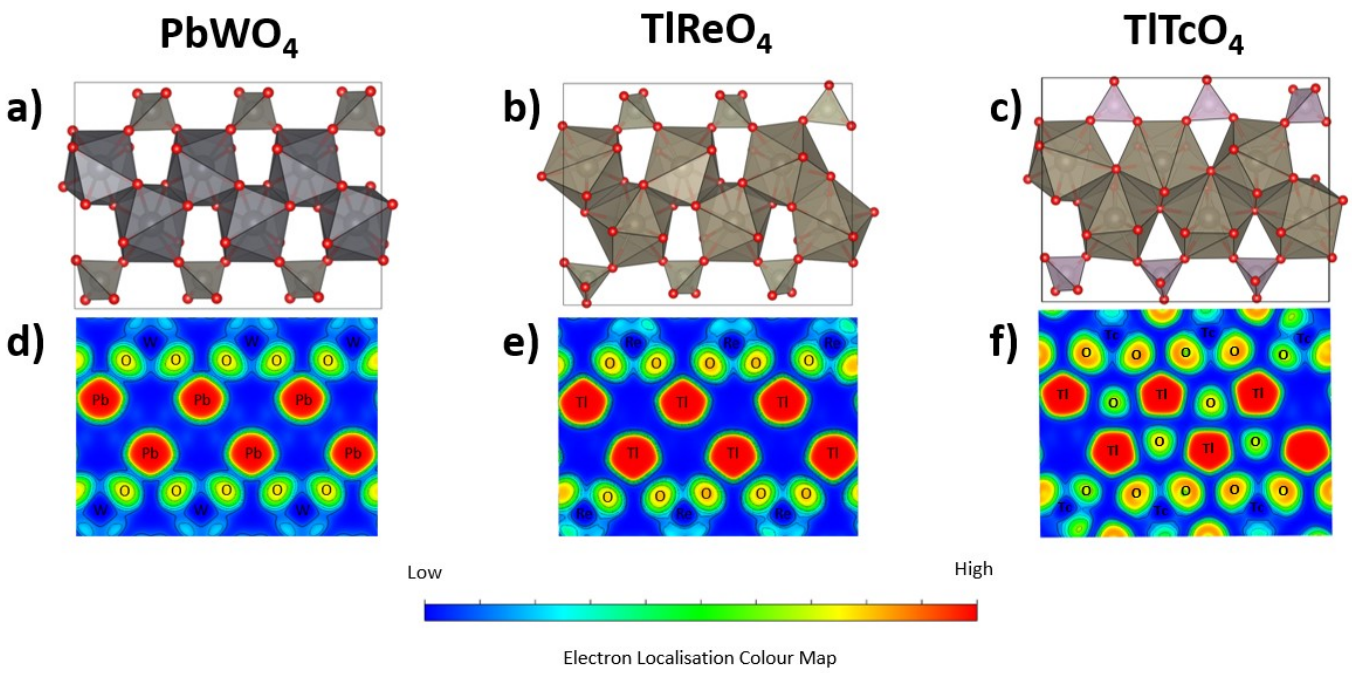

Figure S31: Visualisation of the electron localisation function of (a,d) $PbWO_4$, (b,e) $TlReO_4$. and (c,f) TlTcO4 in the monoclinic $P2_1/c$ model, with the electron localisation of atoms in the <001> plane illustrated. (a-c) Drawn with the polyhedra, and (d-f) drawn with the electron localisation function.

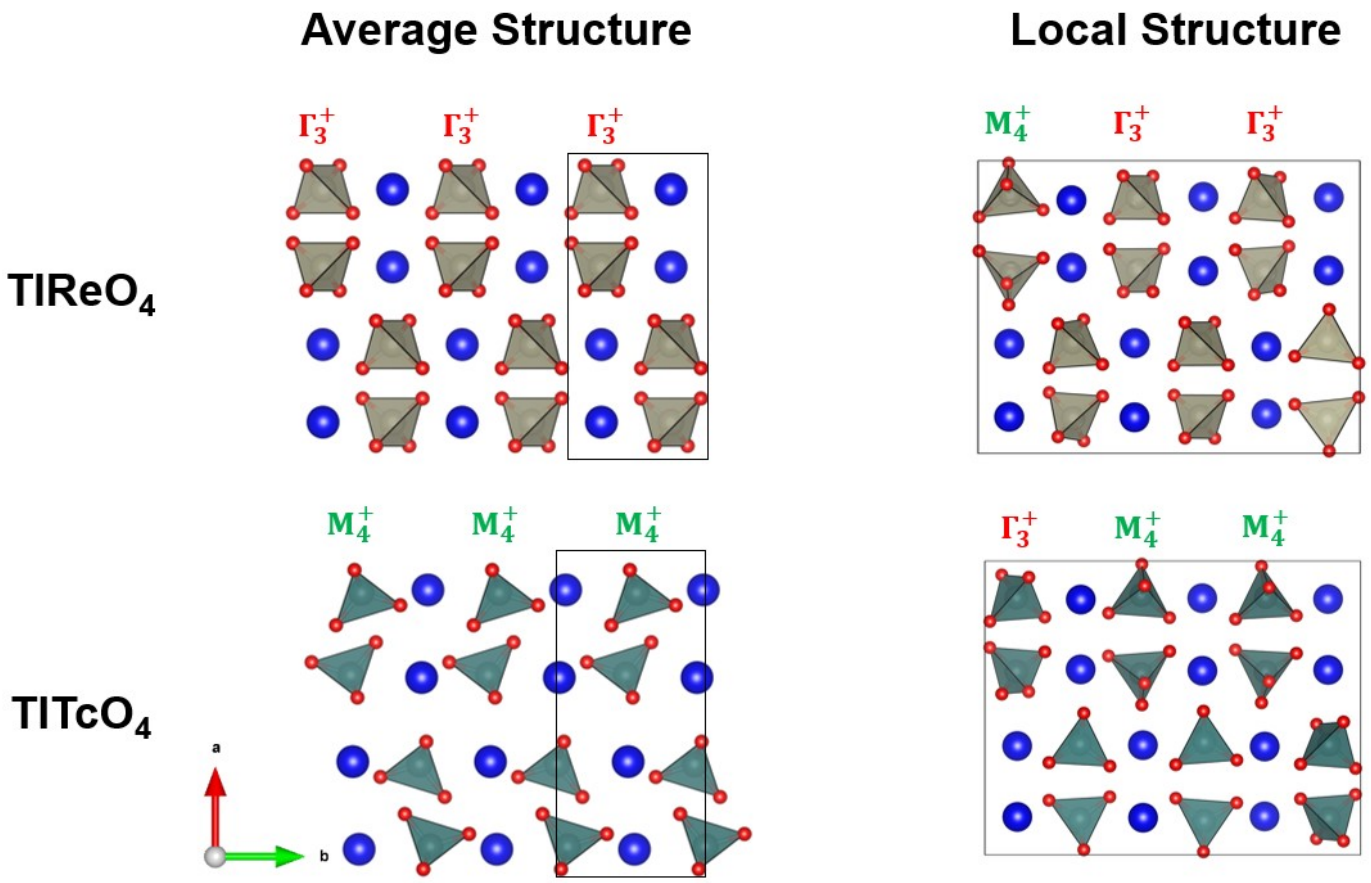

Figure S32: Structures of $TlReO_4$ and $TlTcO_4$ using neutron diffraction and total scattering. The average structure of $TlReO_4$ is tetragonal $I4_1/a$ consisting of ReO_4 tetrahedra rotated by the Γ_3^+ mode. The average structure of $TlTcO_4$ is orthorhombic *Pnma* consisting of TcO_4 tetrahedra rotated by the M_4^+ mode. In the local structure, there appears to be a combination of BO_4 tetrahedra rotated by the Γ_3^+ and M_4^+ modes.

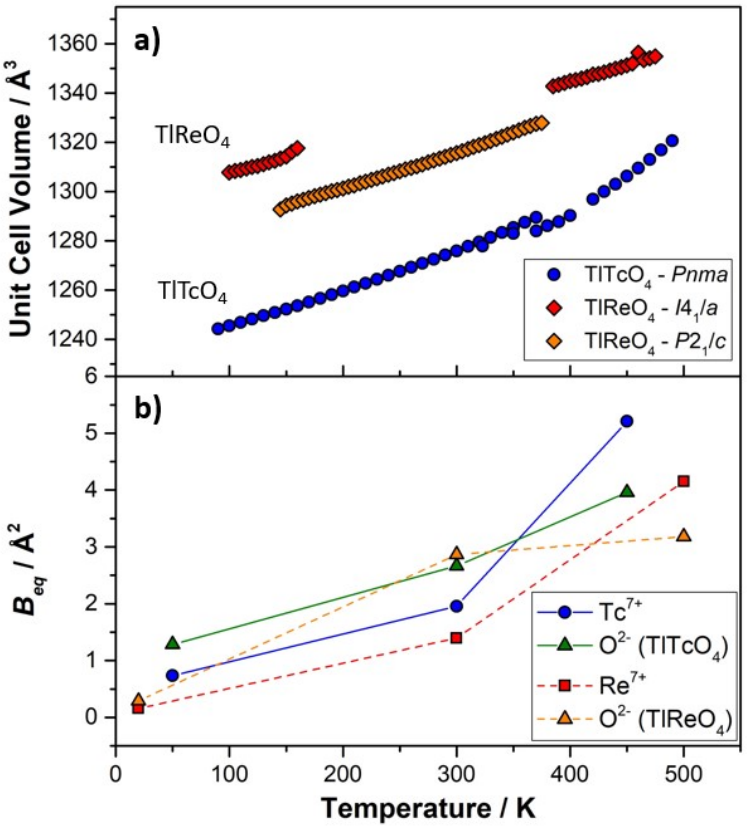

Figure S33: (a) The unit cell volume of $TlTcO_4$ and $TlReO_4$ taken from Kennedy *et al.* and Chay *et al.*, respectively. Data was taken from the Rietveld refinements of synchrotron X-ray diffraction data, with the unit cell volume tripled to allow for a comparison between the orthorhombic *Pnma*, tetragonal $I4_1/a$, and monoclinic $P2_1/c$ structures. (b) The atomic displacement parameters of Tc^{7+} and O^{2-} in $TlTcO_4$ compared with that of Re^{7+} and O^{2-} in $TlReO_4$. Data were derived from the neutron pair distribution function fits to the monoclinic $P2_1/c$ model, and from Saura-Múzquiz *et al.*